Structural state diagram of concentrated suspensions of jammed soft particles in oscillatory shear flow

Fardin Khabaz,[1] Michel Cloitre,[2] and Roger T. Bonnecaze[1,*]
[1]*McKetta Department of Chemical Engineering, University of Texas at Austin, Austin, Texas 78712, USA*
[2]*Soft Matter and Chemistry, CNRS, ESPCI Paris, PSL Research University, 10 Rue Vauquelin, 75005 Paris, France*

(Received 9 November 2017; published 26 March 2018)

In a recent study [Khabaz *et al.*, Phys. Rev. Fluids **2**, 093301 (2017)], we showed that jammed soft particle glasses (SPGs) crystallize and order in steady shear flow. Here we investigate the rheology and microstructures of these suspensions in oscillatory shear flow using particle-dynamics simulations. The microstructures in both types of flows are similar, but their evolutions are very different. In both cases the monodisperse and polydisperse suspensions form crystalline and layered structures, respectively, at high shear rates. The crystals obtained in the oscillatory shear flow show fewer defects compared to those in the steady shear. SPGs remain glassy for maximum oscillatory strains less than about the yield strain of the material. For maximum strains greater than the yield strain, microstructural and rheological transitions occur for SPGs. Polydisperse SPGs rearrange into a layered structure parallel to the flow-vorticity plane for sufficiently high maximum shear rates and maximum strains about 10 times greater than the yield strain. Monodisperse suspensions form a face-centered cubic (FCC) structure when the maximum shear rate is low and hexagonal close-packed (HCP) structure when the maximum shear rate is high. In steady shear, the transition from a glassy state to a layered one for polydisperse suspensions included a significant induction strain before the transformation. In oscillatory shear, the transformation begins to occur immediately and with different microstructural changes. A state diagram for suspensions in large amplitude oscillatory shear flow is found to be in close but not exact agreement with the state diagram for steady shear flow. For more modest amplitudes of around one to five times the yield strain, there is a transition from a glassy structure to FCC and HCP crystals, at low and high frequencies, respectively, for monodisperse suspensions. At moderate frequencies, the transition is from glassy to HCP via an intermediate FCC phase.

DOI: 10.1103/PhysRevFluids.3.033301

I. INTRODUCTION

Measurement of rheological properties during oscillatory shear is a common method of characterization of complex fluids [1,2]. The rheology of course depends on the microstructure of the material. Application of oscillatory shear flow can alter the microstructure of colloidal suspensions and consequently the rheology [3]. Hard sphere suspensions under oscillatory shear flow show a variety of microstructures such as face-centered cubic (FCC), stacked, and tilted layers with a hexagonal close-packed (HCP) configuration and stringlike structure [4–8]. It has been found that when the strain amplitude and the applied frequency is low, colloidal suspensions of hard spheres generally tend to rearrange into the FCC lattice structure. On the other hand, at high frequencies and

*rtb@che.utexas.edu

large amplitudes of oscillations the suspensions form HCP structures [4–8]. In general the formation of these phases depends on the degree of polydispersity, volume fraction, and the flow conditions (i.e., the frequency and strain amplitude). In addition these sheared microstructures are not in equilibrium, and they return to a liquid-like phase on cessation of flow [5,6].

Koumakis *et al.* [9] studied the rheology of monodisperse PMMA hard spheres and showed that these suspensions form crystalline structures. The viscous and elastic moduli of these crystallized suspensions are significantly lower compared to their glassy counterparts. It was also found that under large-amplitude oscillatory shear, the crystallization can occur only if the strain exceeds the yield strain of the material during the oscillation [10]. For colloidal particles with an effective hard sphere volume fraction of 0.62 [7], low frequencies and stress amplitudes lead to a HCP sheetlike structure after flow cessation, while high frequencies and stress amplitudes result in melting of this structure.

While hard sphere glasses experience forces only due to the excluded volume interactions, the soft particles glasses (SPGs) are compressed and interact by pairwise elastic repulsions. The average deformation of the particles depends on the volume fraction and contact modulus of the particles [11]. These suspensions share a similar equilibrium phase diagram with the hard sphere model until they become jammed [12,13]. The glass and jamming transitions occur at volume fraction of about 0.58 and 0.64, respectively. At higher volume fractions, where particles are jammed, the elastic contact forces and imposed shear determine the microstructure and rheology. Brownian forces are negligible compared to the elastic contact forces [14]. A number of experiments have reported ordering of concentrated suspensions of soft particles under shear flow. Paulin *et al.* investigated the response of suspensions of PMMA spherical microgels to oscillatory shear flows with variable frequencies and strain amplitudes [15]. They report out-of-equilibrium phase diagrams which show that above the freezing point amorphous suspensions can be driven into FCC, sliding layer structures, and mixtures depending on the strain amplitude and frequency. Huang and Mason [16] used large-amplitude shear oscillation light scattering [17] to study average droplets' deformation and their microstructure in oil-in-water emulsions. They showed that application of large-amplitude oscillatory shear can induce sliding hexagonal layers in the microstructure, and the ordering depends on the volume fraction and shear history of the sample at the vicinity or above the jamming volume fraction [16]. Very recently [18] it was shown that ultrasoft colloidal star polymers with volume fraction close to the glass line undergo a crystal-to-crystal transition in oscillatory shear flow. In particular it was found that 1,4-polybutadiene stars transform directly from a BCC-dominated phase to an HCP-like microstructure at an intermediate range of Péclet (Pe) numbers. A fluid-to-crystal transformation was observed for large Pe.

In our previous study [19] we used particle-dynamic simulations [14] to explore the microstructure of monodisperse and polydisperse suspensions of jammed SPGs in steady shear flow. Results demonstrated that SPGs with a low degree of polydispersity undergo a phase transition from a glass to an FCC microstructure at low shear rates. This microstructure persists even after flow cessation. Above a critical shear rate, the FCC structure transitions to HCP. Again, if the flow stops, the HCP structure persists. For polydisperse suspensions, a disordered structure is observed at low shear rates, and a layered phase is formed at high shear rates. On cessation of the flow, the particles in the layered structure rearrange to become disordered once again. We also showed that the formation of these layers in the steady shear flow is a shear-activated phenomenon. A dynamic state diagram of the SPGs was determined as a function of the polydispersity and ratio of viscous to elastic forces.

The rheology of materials is often characterized using oscillatory rather steady shear. In this article, we perform numerical simulations to construct a state diagram of the SPGs under oscillatory shear, which is expected to be useful for experimentalists. The simulation is based on the micromechanical framework that has been successfully used to investigate the rheology of SPGs in steady [14,19] and oscillatory [20] shear flows. The state diagram and the dynamics of the microstructures in oscillatory shear simulations are compared with those in steady shear. We show that the monodisperse suspensions form FCC and HCP crystalline structures at low and high frequencies, respectively, and the polydisperse suspensions turn into a layered phase at high frequencies. These structural changes

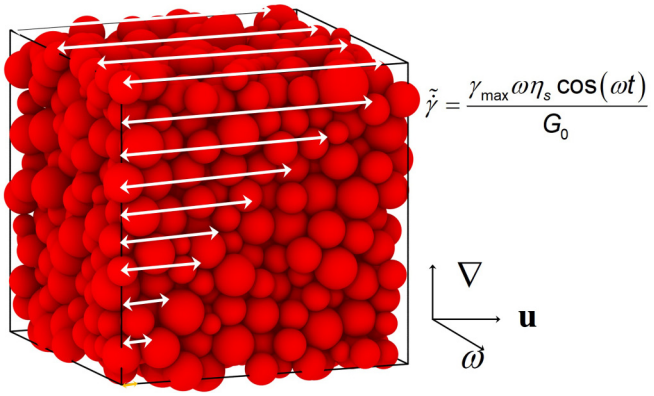

FIG. 1. (a) Configuration of a suspension with a volume fraction of 0.9 and polydispersity index of $\delta = 0.1$ that is in shear flow with an applied frequency of ω and oscillation amplitude of γ_{max}. The flow (**u**), gradient (∇), and vorticity (ω) directions are shown in the figure.

are similar to that seen for steady shear, provided the maximum strain is sufficiently high. However, the dynamics of the structural transitions in oscillatory shear are very different from those in steady shear. In addition the transitions in oscillatory shear do not exhibit an induction strain.

II. SIMULATION METHOD

The soft particle glasses are modeled as suspensions of N non-Brownian elastic particles in a solvent with a viscosity of η_s which are jammed in a cubic simulation box at volume fractions larger than the random close-packing of hard spheres, as shown in Fig. 1 [14,21]. Suspensions with volume fractions of $\phi = 0.7, 0.8,$ and 0.9 are studied. The radii of the particles are assumed to follow a Gaussian distribution with a standard deviation of zero for monodisperse suspensions and values of $\delta = 0.05$, 0.1, and 0.2 for polydisperse suspensions. The average radius of the particles is unity; δ is termed the polydispersity index in the following. The particles are initially placed in a cubic box, and the box size is reduced using Lubachevsky and Stillinger compression algorithm [22]. After reaching the close-packed structure, the spheres are assumed deformable, and the box size is reduced further in small steps. At contact, particles α and β create a flat facet resulting in a deformation of $\varepsilon_{\alpha,\beta} = 0.5(R_\alpha + R_\beta - r_{\alpha\beta})/R_c$, where R_α and R_β are the radii of particle α and β, $r_{\alpha\beta}$ is the center-to-center distance, and R_c is the contact radius, which is given as $R_c = R_\alpha R_\beta/(R_\alpha + R_\beta)$.

Both elastic repulsion and elastohydrodynamic (EHD) forces between particles were considered based on the model proposed by Seth *et al.* [14]. The elastic repulsion force between particles α and β is given by the generalized Hertz law:

$$\mathbf{f}^e_{\alpha\beta} = \tfrac{4}{3} C E^* \varepsilon^n_{\alpha\beta} R_c^2 \mathbf{n}_\perp, \tag{1}$$

where E^* is the particle contact modulus [$E^* = E/2(1-\nu^2)$, with E being the Young modulus, and $\nu = 0.5$ is the Poisson ratio]. C and n are parameters that depend on the degree of compression. For $\varepsilon < 0.1$, $n = 1.5$, and $C = 1$, for $0.1 \leqslant \varepsilon < 0.2$, $n = 3$, and $C = 32$, and if $0.2 \leqslant \varepsilon < 0.6$, $n = 5$, and $C = 790$ [14,23]. $\mathbf{n}_\perp$ is the perpendicular direction to the facet at contact. The EHD drag force, which is due to the existence of a thin film of solvent between the flat facets of two particles in contact during the shear deformation, is given by

$$\mathbf{f}^{\mathrm{EHD}}_{\alpha\beta} = -\left(\eta_s C u_{\alpha\beta,||} E^* R_c^3\right)^{1/2} \varepsilon^{(2n+1)/4}_{\alpha\beta} \mathbf{n}_{||}, \tag{2}$$

where $u_{\alpha\beta,\parallel}$ is the relative velocity component in the direction of $\mathbf{n}_{||}$, which is the direction parallel to the facets at contact. These two forces are assumed to be pairwise additive, and the fluid inertia is

TABLE I. Range of the parameters used in the oscillatory shear simulations of SPGs at different volume fractions.

Parameter	$\phi = 0.7$	$\phi = 0.8$	$\phi = 0.9$
$\tilde{\omega} = \frac{\omega \eta_s}{E^*}$	10^{-8}–10^{-3}	10^{-8}–10^{-3}	10^{-8}–10^{-3}
G_0/E^* [14]	0.00466	0.0281	0.08
$\tilde{\dot{\gamma}}_{\max} = \frac{\omega \eta_s}{G_0}\gamma_{\max}$	6.44×10^{-9}–4.29	1.07×10^{-9}–7.12×10^{-1}	3.75×10^{-10}–2.5×10^{-1}
γ_y [14]	0.032	0.033	0.0472
$\gamma_{\max}/\gamma_y$	0.09–606	0.09–606	0.06–423.7

neglected [14,20]. The suspension is subject to an oscillatory shear flow of the following form [20]:

$$\mathbf{u}_\infty = \frac{\gamma_{\max}\omega\eta_s y \cos(\omega t)}{E^*}\mathbf{e}_x, \tag{3}$$

where $\gamma_{\max}$ is the maximum strain in each oscillation cycle with an applied frequency of ω, and $\mathbf{e}_x$ is the unit vector in the flow direction. The frequency is nondimensionalized by $\tilde{\omega} = \frac{\omega\eta_s}{E^*}$. It ranges from 10^{-8} to 10^{-3}, and the oscillatory flow is applied for 500 oscillation cycles. The dimensionless equation of motion (length, time, and velocity are nondimensionalized by R, η_s/E^*, and RE^*/η_s, respectively) for each particle can be written as

$$\frac{d\mathbf{x}_\alpha}{dt} = \mathbf{u}_\alpha^\infty + \frac{f_r(\phi)}{6\pi R_\alpha}\left[\frac{4}{3}C\sum_\beta \varepsilon_{\alpha\beta}^n R_c^2 \mathbf{n}_\perp - \sum_\beta \left(C u_{\alpha\beta,||} R_c^3\right)^{1/2} \varepsilon_{\alpha\beta}^{(2n+1)/4}\mathbf{n}_{||}\right], \tag{4}$$

where $\mathbf{x}_\alpha$ is the position of the particle α and $f_r(\phi)$ is the mobility function, which was set to 0.01 in the simulations [14,20].

A total number of 10^3 or 10^4 particles are used to simulate the microstructure and induction period of the phase transition (no significant change in the stress-strain curve of these SPGs was seen above 1000 particles). The conditions for the simulations are summarized in Table I. If the strain amplitude is smaller than the yield strain of these materials, the microstructure will preserve its initial disordered state. We note that the three dimensionless groups characterizing the system are the volume fraction ϕ, polydispersity δ, and dimensionless maximum shear rate $\tilde{\dot{\gamma}}_{\max}$. In the following, we will characterize the maximum shear rate by the dimensionless parameter $\tilde{\dot{\gamma}}_{\max} = \frac{\omega\eta_s}{G_0}\gamma_{\max}$, where G_0 is the low-frequency modulus of the suspensions.

Bond order parameters were utilized to characterize the crystal structure of the monodisperse systems studied [19,24]. A bond is defined as a connection between particles i and j that are within a cutoff distance, which here is assumed to be 2.20. The local bond order parameter Q_{lm} is defined as

$$Q_{lm}(\mathbf{r}) \equiv Y_{lm}(\theta(\mathbf{r}),\phi(\mathbf{r})), \tag{5}$$

where $\mathbf{r}$ is the bond between the neighboring particles, $\theta(\mathbf{r})$ and $\phi(\mathbf{r})$ are the polar and azimuthal angles, respectively, and Y_{lm} are the spherical harmonics. The average bond order can be determined by averaging the local bond order parameters over the number of bonds (N_b) in the system:

$$\bar{Q}_{lm} \equiv \frac{1}{N_b}\sum_{\text{bonds}} Q_{lm}(\mathbf{r}). \tag{6}$$

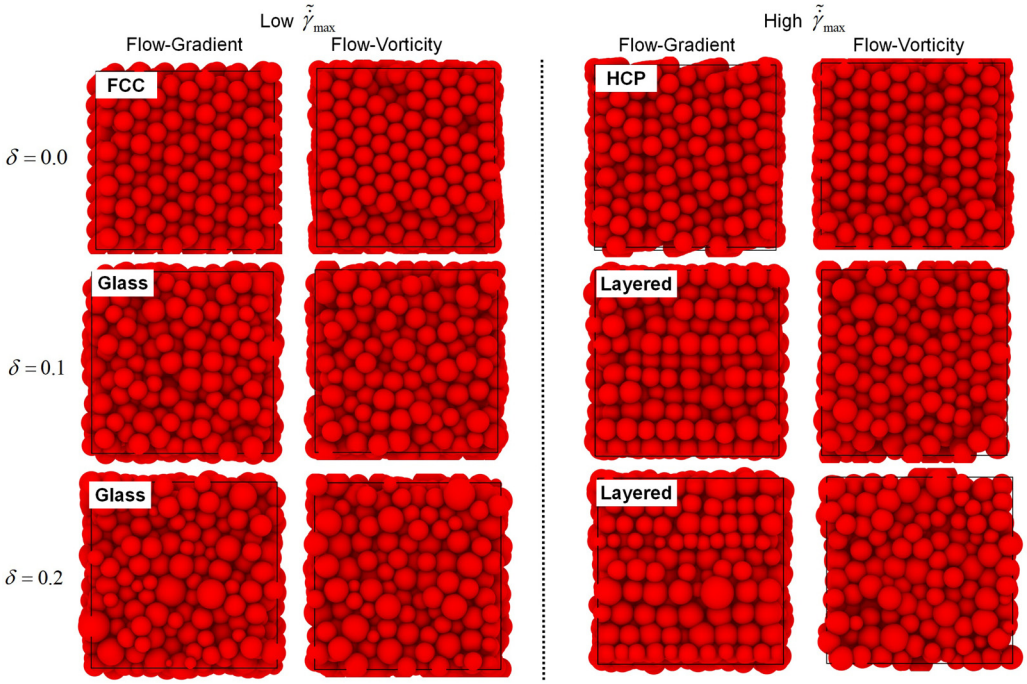

FIG. 2. Snapshot of simulation box of soft particle glasses under low (left) $\tilde{\dot{\gamma}}_{max} = 1.78 \times 10^{-7}$ ($\tilde{\omega} = \omega\eta_s/E^* = 10^{-8}$) and high (right) $\tilde{\dot{\gamma}}_{max} = 0.00178$ ($\tilde{\omega} = \omega\eta_s/E^* = 10^{-4}$) maximum shear rate after 200 cycles. The strain amplitude of the oscillations is $\gamma_{max}/\gamma_y = 10$. The polydispersity δ increases from top to bottom.

To eliminate the dependence of bond order parameters on the rotation of the frame of reference, we calculate the second-order (Q_l) invariant as

$$Q_l \equiv \sqrt{\frac{4\pi}{2l+1}\sum_{m=-l}^{l}|\bar{Q}_{lm}|^2}. \tag{7}$$

The value of the bond order parameter Q_l for an amorphous liquid is zero, and it is nonzero for even values of l when the structure has some degrees of crystallinity. We use the Q_6 bond order parameter to determine the crystal structure [24]. This parameter provides a quantitative metric to determine whether a crystalline structure for monodispersed suspensions is hexagonally closed-packed (HCP) or face-centered cubic (FCC). The Q_6 values for perfect HCP and FCC crystals are 0.48 and 0.57, respectively [19].

Structural properties of the system were characterized by determining the pair distribution function in suspensions with $N = 10^4$ particles. The pair distribution functions $g_{u\nabla}(\rho)$ and $g_{u\omega}(\rho)$ in the flow-gradient and flow-vorticity planes were computed at different strain values and frequencies to investigate the structural rearrangement as a function of the simulation time. Here ρ is the magnitude of the two-dimensional position vector of a given particle in the flow-gradient and flow-vorticity planes that is normalized by the radius of the particle.

III. RESULTS AND DISCUSSION

A. Microstructure of monodisperse suspensions

Snapshots of suspensions at a volume fraction of 0.8 in the simulation box at low ($\tilde{\dot{\gamma}}_{max} = 1.78 \times 10^{-7}$) and high ($\tilde{\dot{\gamma}}_{max} = 0.00178$) maximum shear rates are shown in Fig. 2 for SPGs of different

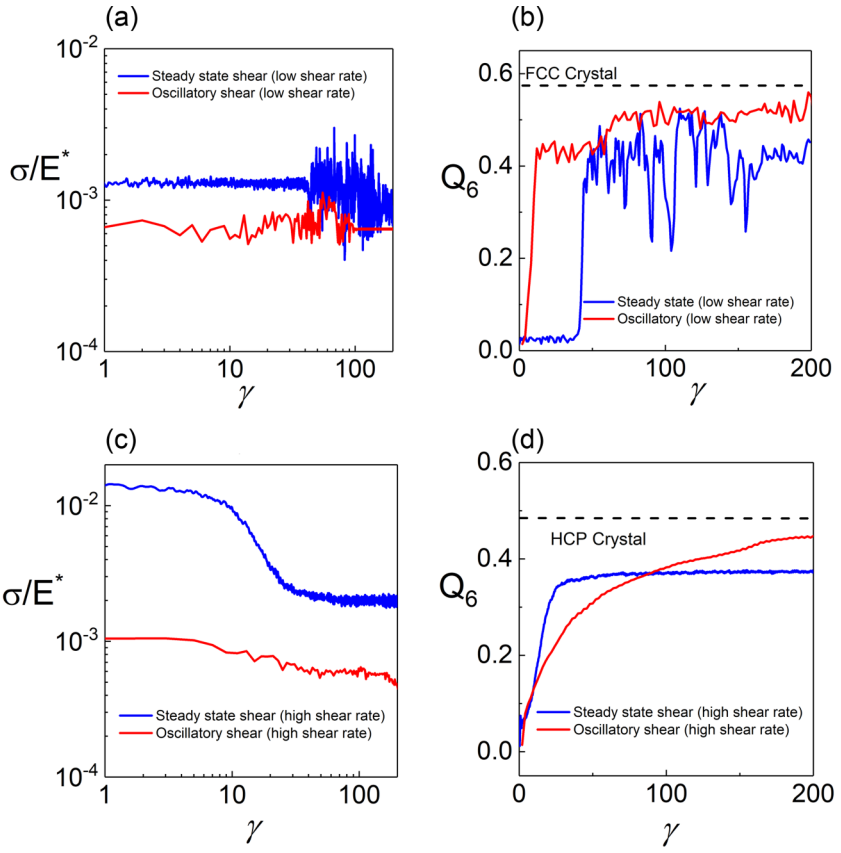

FIG. 3. Shear stress (a), (c) and bond order parameter Q_6 (b), (d) for monodisperse suspensions under steady and oscillatory shear flows as a function of strain. The horizontal dashed lines show the values of these parameters for perfect FCC and HCP crystals. The applied strain amplitude γ_{max}/γ_y is 10, and the applied frequencies are $\tilde{\omega} = \omega\eta_s/E^* = 10^{-8}$ (top panels) and $\tilde{\omega} = \omega\eta_s/E^* = 10^{-4}$ (bottom panels), which correspond to maximum shear rates of $\tilde{\dot{\gamma}}_{max} = 1.78 \times 10^{-7}$ and $\tilde{\dot{\gamma}}_{max} = 0.00178$, respectively. The volume fraction of suspension is $\phi = 0.8$.

polydispersity indexes. The strain amplitude in both cases is $\gamma_{max} = 0.5$, which is about 10 times greater than the yield strain of the SPG. After 200 oscillations, the structures of the initially disordered monodisperse suspensions become FCC or HCP at low or high frequencies, respectively. As the polydispersity increases to 0.1, suspensions preserve their glassy structures at the lower maximum shear rate. On the other hand, layered microstructures are formed at the high maximum shear rate. These layers are parallel to the flow-vorticity plane. At a polydispersity of 0.2, the microstructure shows a weaker degree of the ordering compared to the polydispersity of 0.1. The same structural transitions occur for suspensions at other volume fractions. These structures are similar to recent simulations of these suspensions in steady shear flow [19].

In order to quantify the microstructure and rheology of the monodisperse suspensions, the shear stress and bond order parameters (BOPs) Q_6 were calculated [19,24] as a function of the simulation time or strain. In order to compare the stress-strain behavior in oscillatory shear simulations with steady state results, the average of absolute values of the shear stress in each oscillation was computed and plotted against the strain. Results are shown in Fig. 3 for a monodisperse suspension with a volume fraction of 0.8. At a low shear rate, the shear stress of monodisperse suspension in steady shear simulations initially is constant, and then it shows fluctuations at high strain values. These

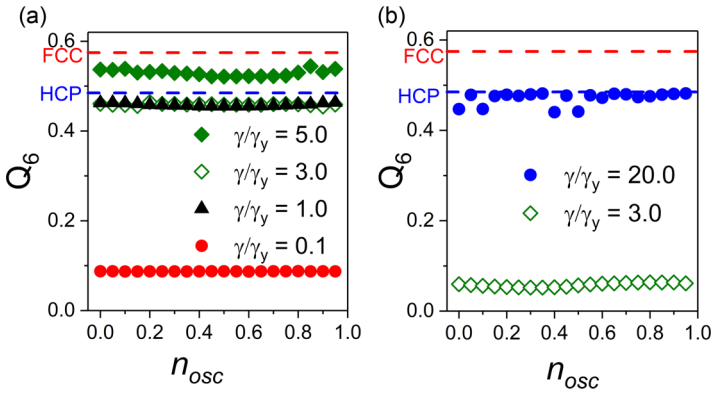

FIG. 4. Variation of the Q_6 parameter during a single oscillation in (a) a low frequency of $\tilde{\omega} = \omega\eta_s/E^* = 10^{-8}$ and (b) a high frequency of $\tilde{\omega} = \omega\eta_s/E^* = 10^{-4}$ for monodisperse suspension with a volume fraction of 0.8. For the low-frequency oscillation, the transition from a glass to an HCP structure occurs at $\gamma_{\max}/\gamma_y = 1$. For high-frequency oscillation, this transition requires the maximum strain amplitude $\gamma_{\max}$ to be much greater than the yield strain γ_y.

fluctuations are due to the appearance of defects in the FCC crystalline structure. On the other hand, in oscillatory shear simulations, stress initially shows fluctuations and then it reaches a constant value. As seen in Fig. 3(b), the values of Q_6 for a monodisperse suspension sheared at a shear rate of $\tilde{\dot{\gamma}}_{\max} = 1.78 \times 10^{-7}$ are around 0.40 in the steady shear flow, which are slightly different from the values expected for a perfect FCC lattice. In the oscillatory shear flow, at the same maximum shear rate, the value of Q_6 is around 0.50, which is in a good agreement with the value of a perfect FCC crystal. At a high shear rate, the shear stress in the steady shear simulations shows a plateau region during the induction period [19] up to a strain value of 10, and then decreases to a steady state, while the stress continuously decreases and reaches a steady state value at high strain values in the oscillatory shear flow. Furthermore, as seen in Fig. 3(d), Q_6 is around 0.36 in the steady shear flow that is smaller than the value of perfect HCP lattice [24]. By contrast oscillatory shear flow results in the formation of a better HCP-like structure; the value of $Q_6 \cong 0.44$ is in a good agreement with that of a perfect HCP crystal.

In both steady and oscillatory shear flows, the microstructure of the monodisperse suspensions shows a FCC crystalline structure at low maximum shear rates. An increase in $\tilde{\dot{\gamma}}_{\max}$ leads to a formation of an HCP-like microstructure [19]. This behavior is also seen for other volume fractions. In all cases, the quality of the shear-induced lattice is significantly better in terms of fewer defects in the oscillatory shear flow compared to the steady state flow. We attribute this observation to the annealing character of the oscillatory shear flow [3,25].

In order to investigate the effect of the strain amplitude (specially close to the yield point of the suspensions) on the microstructure of the monodisperse suspensions in an oscillation cycle, we have determined the bond order parameter of Q_6 during a cycle as seen in Figs. 4(a) and 4(b) at low and high maximum shear rates, respectively, for a suspension with a volume fraction of 0.8. At a low shear rate of $\tilde{\dot{\gamma}}_{\max} = 1.78 \times 10^{-7}$, when the strain amplitude is less than the yield strain of the material i.e., $\gamma_{\max}/\gamma_y = 0.1$, the microstructure remains glassy. In this case as expected, the Q_6 parameter is close to zero revealing the amorphous nature of the suspension. As the strain amplitude increases ($\gamma_{\max}/\gamma_y = 3$), this parameter increases to the limiting value for an HCP lattice. A further increase of the strain amplitude leads to the formation of the FCC lattice at low frequencies as seen for $\gamma_{\max}/\gamma_y = 5$. On the other hand, when the frequency is $\tilde{\omega} = \omega\eta_s/E^* = 10^{-4}$ the Q_6 parameter is close to zero, and the microstructure remains glassy during a cycle of oscillation when the strain amplitude is small. This observation occurs up to a strain value of $\gamma_{\max}/\gamma_y = 3$ as shown in Fig. 4(b). A further increase in the strain amplitude leads to the formation of HCP microstructure. In all cases

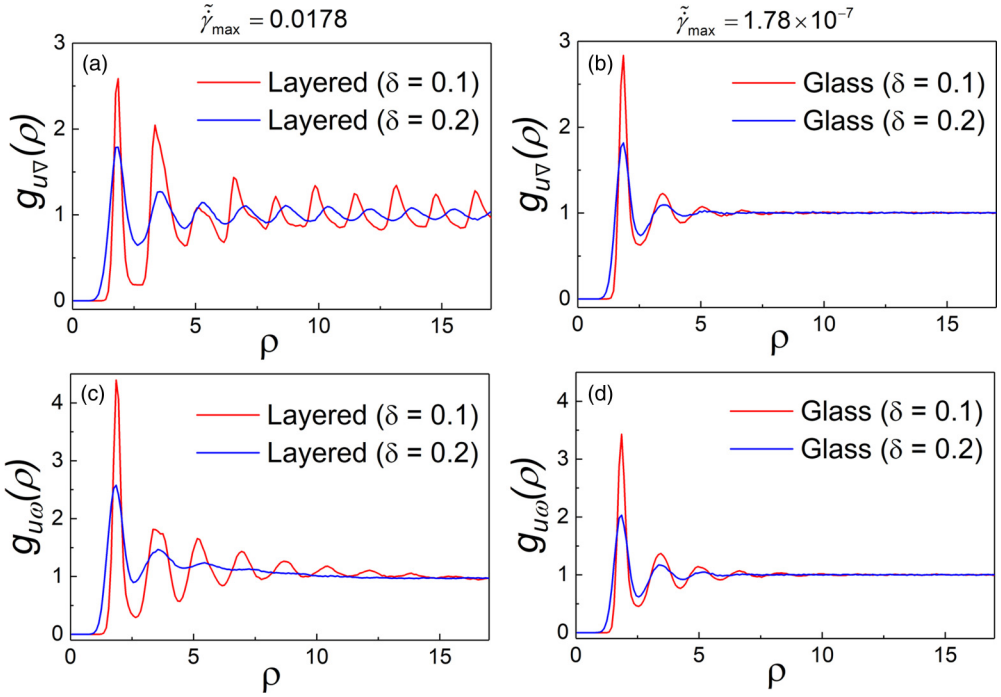

FIG. 5. Pair distribution functions in the flow-gradient (a) and (b) flow-vorticity (c) and (d) planes for the glassy and layered suspensions at a high [(a) and (c); $\tilde{\dot{\gamma}}_{max} = 1.78 \times 10^{-2}$ and $\gamma_{max}/\gamma_y = 10$] and a low [(b) and (d); $\tilde{\dot{\gamma}}_{max} = 1.78 \times 10^{-7}$ and $\gamma_{max}/\gamma_y = 10$] maximum shear rate.

the suspension shows a uniform lattice microstructure in a cycle of oscillation and the lattice structure is not a function of the oscillation time. In particular we do not observe melting of the crystallized or layered suspensions. Experimentally, it was shown that a concentrated solution of triblock copolymer poly(ethylene oxide)$_{106}$-poly(propylene oxide)$_{68}$-poly(ethylene oxide)$_{106}$ (Pluronic F127) crystallizes and melts in a cyclic fashion under large amplitude oscillatory shear experiments [26]. The volume fraction of the sample in this experimental study was around 0.28 [27], which is significantly smaller than the required value for jamming transition in SPGs. At this low volume fraction ($\phi = 0.28$), the Brownian motion is important that is not captured or important in our model for SPGs.

B. Microstructure of polydisperse suspensions

In order to analyze the microstructure of the polydisperse suspensions, we computed the two-dimensional (2D) distribution functions in the flow-gradient [$g_{u\nabla}(\rho)$] and flow-vorticity [$g_{u\omega}(\rho)$] directions [19] for SPGs that form either layered and glassy structures under oscillatory shear deformation. Layering occurs at high shear rate, and the glassy structure is preserved at low shear rate. As shown in Fig. 5(a), the distribution functions of polydisperse suspensions in the flow-gradient plane shows distinct peaks over extended distances at a shear rate of $\tilde{\dot{\gamma}}_{max} = 0.0178$. Similarly, in the flow-vorticity plane as seen in Fig. 5(c), ordered microstructures are observed. This ordering is more like a formation of hexagonal pattern with some defects, which was also seen in the steady shear simulations [19]. These observations indicate the formation of layers parallel to the flow-vorticity plane. The degree of ordering is weaker inside the flow-vorticity plane of the suspension with the highest degree of polydispersity as the peaks disappear at $r \approx 12\,\mathrm{R}$. On the other hand, when the maximum shear rate is low ($\tilde{\dot{\gamma}}_{max} = 1.78 \times 10^{-7}$), the distribution functions indicate that the liquid-like structure is preserved in the oscillatory shear flow. As mentioned earlier, the applied

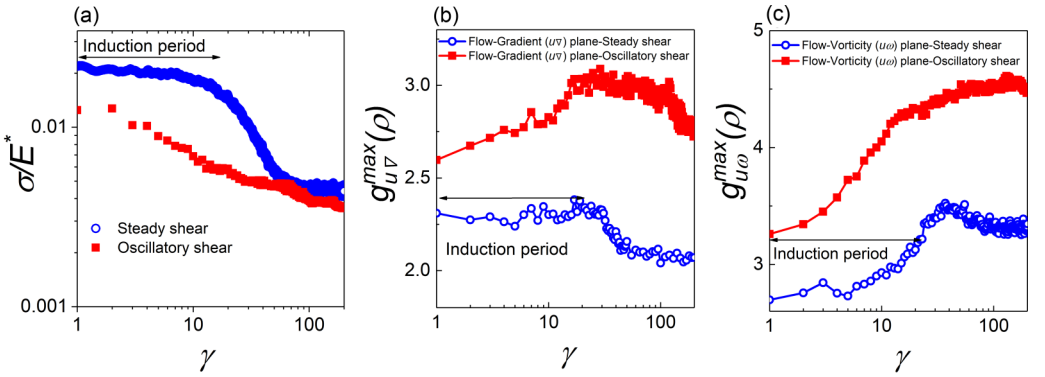

FIG. 6. (a) Shear stress and the maximum of pair distribution function in (b) flow-gradient and (c) flow-vorticity planes as a function of the strain. The maximum shear rate is $\tilde{\dot{\gamma}}_{\max} = 0.0178$, and the strain amplitude is $\gamma_{\max}/\gamma_y = 10$. The volume fraction of the suspension is 0.8 and the polydispersity index is 0.1.

strain amplitude must be larger than the yield strain of the suspension, otherwise the suspension will preserve its initial microstructure (simulations with a layered starting configuration were performed to confirm this phenomenon).

In order to find the similarities and differences between the layering in the steady and oscillatory shear flows, the shear stress was compared as a function of the strain at a high shear rate. As shown in Fig. 6(a), in the steady shear, the stress is constant during the induction period and then decreases and reaches a steady state value at high strains [19]. This decrease in the shear stress coincides with the transformation of the microstructure from a glassy to a layered state. The evolution of the stress in oscillatory shear is distinctly different. It decreases continuously and takes a larger number of strains to reach a steady-state value.

The maximum values of the 2D pair distribution functions in the flow-gradient and flow-vorticity planes were also determined as a function of the strain to show the difference in the evolution of the microstructure in steady and oscillatory shear flows of polydisperse suspensions. The maximum of the distribution function in the flow-gradient plane during the stress plateau in steady shear flow remains constant and decreases to a steady state value after layering as it was observed in our previous study [see Fig. 6(b)]. In oscillatory shear this parameter increases and then decreases to a steady state value. In Fig. 6(c) the maximum of the flow-vorticity pair distribution function is plotted against the strain. In both cases the rearrangements of the microstructure occur continuously until the layered structure is formed. As noted earlier, the microstructure is glassy at low frequencies and is independent of the strain amplitude. The shear stress is constant as a function of the strain in both steady state and oscillatory shear, and the maximum of the flow-gradient and flow-vorticity distribution function does not change as a function time, which confirms that the suspensions remain in a glassy state.

C. Dynamic state diagrams

Using the quantitative microstructural parameters, we constructed a state diagram of the SPGs in the oscillatory shear flow for maximum strain amplitudes greater than the yield strains. The microstructure of the suspension is determined by its polydispersity, maximum strain, and shear rate $\tilde{\dot{\gamma}}_{\max} = \omega\eta_s\gamma_{\max}/G_0$. The state diagrams are shown in Figs. 7(a)–7(c) for volume fractions of 0.7, 0.8, and 0.9, respectively. As illustrated in Fig. 2, the monodisperse suspensions form FCC-like lattices at low shear rates, and they transform into HCP-like microstructures at higher shear rates. This phase change for different suspensions occurs at approximately $\tilde{\dot{\gamma}}_{\max} = 2 \times 10^{-5}$–$4 \times 10^{-5}$, which is in very close agreement with our previous steady shear simulations [19], which showed a transition around $\tilde{\dot{\gamma}}_{\max} = 3 \times 10^{-5}$. For polydisperse suspensions, the glassy structure is preserved at low shear

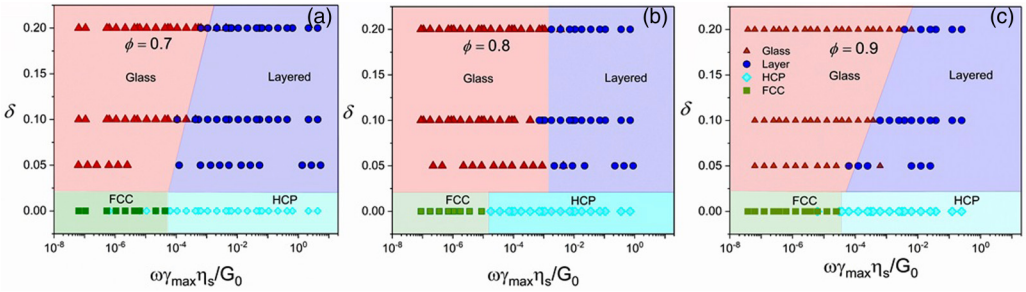

FIG. 7. The state diagram of the SPGs at a volume fraction of (a) 0.7, (b) 0.8, and (c) 0.9 in the oscillatory shear flow. The lowest relative strain used to construct the state diagram is $\gamma_{\max}/\gamma_y = 3$.

rates, while the structure becomes layered at high shear rates. We note that as the polydispersity increases for volume fractions of 0.7 and 0.9, the onset of the layering shifts to higher shear rates. The transition to the layered phase occurs over a shear rate range of $\tilde{\gamma}_{\max} = 8 \times 10^{-4} - 5 \times 10^{-3}$ depending on the volume fraction of the suspension. This is slightly different from our observation in steady shear flow, where the border between the glassy and layered phases was almost a vertical line around a shear rate of 10^{-3} [19].

The state of the SPGs in oscillatory shear flow depends on both applied oscillation frequency and strain amplitude. To understand the behavior of SPGs close to the yield point, we have constructed dynamical state diagrams for two extreme cases (i.e., monodisperse and polydisperse suspension with $\delta = 0.2$ at different volume fractions) in Figs. 8(a) and 8(b). Monodisperse suspensions at low frequencies show a glassy microstructure when the strain amplitude is smaller than the yield strain. At a fixed frequency, increasing the strain amplitude leads to the formation of the FCC microstructure. At intermediate frequencies and high strain amplitudes, we also see a transformation from FCC to HCP crystalline structures. Furthermore, at high frequencies, the transformation directly happens from a glassy structure to HCP phase upon increasing the strain amplitude. We note that some of the simulations show a polycrystalline phase (i.e., mixture of FCC and HCP) at the vicinity of the

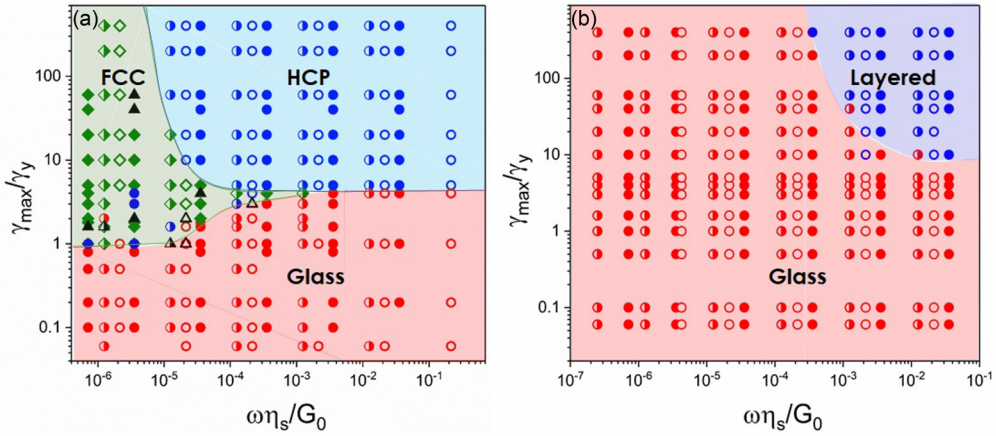

FIG. 8. The state diagram of the (a) monodisperse and (b) polydisperse ($\delta = 0.2$) SPGs at different volume fractions. The following symbols are used to distinguish the state of SPGs with different volume fraction: $\phi = 0.7$: glass (○), FCC (◇), HCP (○), and FCC-HCP mixture (△). $\phi = 0.8$: glass (●), FCC (◆), HCP (●), and FCC-HCP mixture (▲). $\phi = 0.9$: glass (◑), FCC (◈), HCP (◑), and FCC-HCP mixture (◭). For a layered phase in monodisperse SPGs the same symbols as the HCP phase in monodisperse SPGs are used.

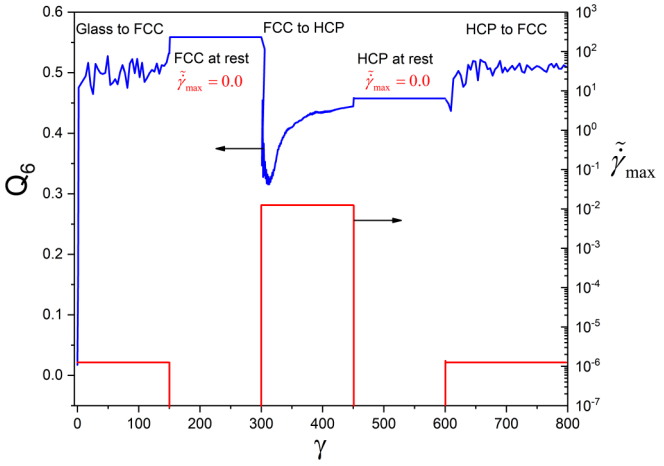

FIG. 9. The bond order parameter Q_6 (left axis) and maximum shear rate (right axis) as a function of strain for a suspension with a volume fraction of 0.9. The initial configuration of the suspension, i.e., at $\gamma = 0$ is a glass. When the suspension is at rest: $\tilde{\dot{\gamma}}_{max} = 0$.

borderlines for these crystalline structures, which can be due to a system size effect. Finally there is a limited domain of the phase diagram located at low strain amplitudes and low frequency where the oscillatory shear flow melts the FCC crystalline structure into a disordered state. On the other hand, polydisperse suspensions form amorphous microstructures at all strain amplitudes at low frequencies. As seen in Fig. 8(b), the layered phase is formed only at high frequencies and large strain amplitudes at all volume fractions.

Paulin *et al.* [15] performed oscillatory shear experiments on close to monodisperse swollen PMMA microgels. Using light scattering in the vorticity-velocity plane, they observed the transition of the suspension from a glass to FCC to so-called sliding layer structures with increasing strain. The prediction in Fig. 8(a) of the transition from a glass to crystalline structure for sufficient strain is consistent with these experimental observations. For intermediate shear rates, the glass is predicted to go first to FCC and then HCP, sliding layer, with increasing strain.

IV. DISCUSSION: STABILITY AND REVERSIBILITY OF THE SHEAR-INDUCED STRUCTURES

As mentioned earlier if the maximum strain is less than the yield strain, the microstructural state of the system remains unchanged from the initial jammed state. For the monodisperse suspensions, there is no transition from FCC to HCP and the microstructure is always glassy. Similarly no layered phase was observed for the polydisperse suspensions when the strain amplitude was less (or slightly larger) than the yield strain. As in the steady shear simulations, the stability and reversibility of these microstructures under oscillatory shear flow were examined. Starting from a glassy structure of monodisperse suspensions, given the strain amplitude is larger than the yield strain of the material, at low frequencies particles rearrange into a FCC-like lattice, and at high frequencies they form a HCP-like crystal. In order to investigate the stability of these crystals, the shear flow was switched off, and the microstructure of the monodisperse suspensions was analyzed as a function of the simulation time. As seen in Fig. 9, for a suspension with a volume fraction of 0.9, the Q_6 parameter initially increases from zero when the suspension is subjected to the oscillatory shear flow (with a low frequency) and reaches a value of 0.52, which confirms the formation of a FCC lattice. At this point, when the suspension is kept at rest (i.e., no flow), the particles first rearrange slightly so that the Q_6 parameter increases to a value of 0.56, which is in a close agreement with a value of 0.57 for a perfect FCC lattice, and then the microstructure remains unchanged in time. Let us now subject the FCC structure obtained at rest to a high-frequency oscillatory shear flow as seen in

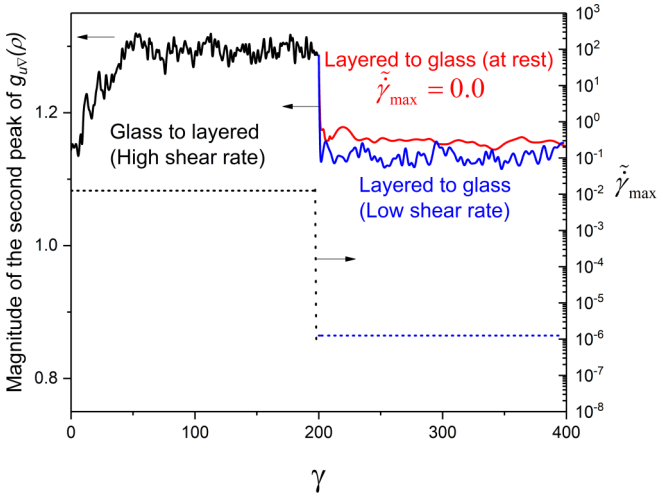

FIG. 10. Magnitude of the second peak of the $g_{u\nabla}(\rho)$ (left axis) and the maximum shear rate (right axis) as a function of the strain. The suspension has a volume fraction of 0.9 and polydispersity index of 0.2. The initial state $\gamma = 0$ is a glassy structure. When the suspension is at rest, $\tilde{\dot{\gamma}}_{max} = 0$. The shear rate evolution is shown with a dotted line.

Fig. 9. In this high-frequency regime, the Q_6 parameter decreases to a value of 0.48, which indicates that the microstructure becomes HCP. The HCP microstructure is also stable and ceasing the flow does not alter the lattice structure. As seen in the figure, the Q_6 parameter is constant after flow cessation once the transition to HCP occurs. Finally, the HCP-like crystal obtained after flow cessation transforms into a FCC-like crystalline structure when subjected to low frequencies as the bond order parameters become very close to the limits of the FCC crystalline lattice. The important point here is that the transformation from FCC-to-HCP (and HCP-to-FCC) occurs without any intermediate amorphous step. This finding is in agreement with the recent study by Ruiz-Franco *et al.* [18] that showed that ultrasoft star polymers close to the glass transition packing undergo crystal-to-crystal transition without any intermediate step in steady and oscillatory shear flow at a moderate Pe number range. Furthermore, we checked that the FCC and HCP crystalline microstructures produced by applying a large strain $\gamma_{max}/\gamma_y = 10$ are preserved when subjected to small amplitude oscillatory shear simulations (results are not shown here).

While the transformations from HCP to FCC and vice versa occur relatively fast for monodisperse suspensions upon reducing or increasing the oscillation frequency, the polydisperse suspensions show a different behavior. The 2D distribution function is a great indicator of the formation of a layered microstructure in shear flow. This distribution function shows several peaks at large distances between the reference particle and the test particle due to the formation of layers parallel to the flow-vorticity plane. Here we only track the magnitude of the second peak of $g_{u\nabla}(\rho)$ as a function of the strain applied to the suspension as shown in Fig. 10. Initially when the glassy suspension is subjected to the high-frequency oscillations ($\tilde{\omega} = \frac{\omega\eta_s}{E^*} = 10^{-4}$), the value of the second peak increases and reaches a constant value. At this point, the layered structure is subjected to two independent simulations. In one case a low frequency of $\tilde{\omega} = \frac{\omega\eta_s}{E^*} = 10^{-8}$ is applied to the suspension, and as seen in the figure the value of the second peak declines to the original value of an amorphous suspension. This behavior shows that the layering phenomenon is reversible for polydisperse suspensions. We also note that as strain increases, the layers start disappearing and the magnitude of the peaks at larger distances decrease too. Similarly, in the second case the oscillatory shear flow was turned off (see the red line), and the magnitude of the second peak declines and reaches a value which is close to that of a glassy suspension. A similar behavior also was seen for the flow-vorticity pair distribution function (results

are not shown). These observations demonstrate that the shear-induced layered microstructure is not a stable configuration.

V. SUMMARY AND CONCLUDING REMARKS

We have shown that jammed SPGs can form a variety of microstructures in oscillatory shear flow. Similar to steady shear flow [19], the monodisperse suspensions transform into FCC-like and HCP-like phases at low and high maximum shear rates, respectively, when the amplitude of the strain is larger than the yield strain of the material. On the other hand, the polydisperse suspensions form a layered phase at high frequencies. A dynamic state diagram, which relates the state of these suspensions under oscillatory shear flow to processing parameters such as particle volume fraction, polydispersity, and elasticity and the flow properties like the amplitude of frequency and viscosity, is provided that is in agreement with the state diagram obtained in the steady shear simulations.

These transitions observed in the monodisperse and polydisperse suspensions are reversible. The FCC crystals obtained at low-frequency regime can be turned into HCP-like phases by subjecting the FCC crystals to high frequencies and vice versa. Similarly, a layered phase obtained in the high-frequency regime in polydisperse suspensions transforms into an amorphous structure when the shear rate decreases. Our results clearly show that the monodisperse crystals (i.e., FCC and HCP-like crystals) obtained in oscillatory shear flow are stable and flow cessation does not change their microstructures, while the layered phase in polydisperse suspensions turns into a glassy phase upon flow cessation. The out-of-equilibrium nature of the layered phase has been reported in experiments in the case of dense emulsions [28].

Another important parameter that emerges from our study is the polydispersity. It is striking that jammed suspensions with a polydispersity as high as 20% can order under flow into layered microstructures. This suggests that it would be useful to carefully revisit the current literature on the subject and prompt for future experiments with well-characterized particle size distributions. Other open questions concern the role of Brownian motion and the form of the repulsive interparticle potential. This might explain why ultrasoft star polymers exhibit a BCC crystalline structure at low shear rates and not the FCC symmetry described in this work [18].

In conclusion, subjecting amorphous jammed suspensions to oscillatory shear flows is a powerful tool to assist the design of materials with a desired microstructure. Oscillatory shear can generate FCC and HCP crystals which are much less defective than in steady shear flows. Layered structures can be fabricated, but they need to be rapidly quenched upon flow cessation to maintain their organization. Our hope is that the results reported here will provide guidelines to experimentalists and material scientists to develop tailored colloidal materials.

ACKNOWLEDGMENTS

F.K. and R.T.B. gratefully acknowledge partial support from NSF Grant CBET 1336852. We thank Tianfei Liu for her helpful comments and suggestions during the manuscript preparation.

[1] K. Hyun, M. Wilhelm, C. O. Klein, K. S. Cho, J. G. Nam, K. H. Ahn, S. J. Lee, R. H. Ewoldt, and G. H. McKinley, A review of nonlinear oscillatory shear tests: Analysis and application of large amplitude oscillatory shear (LAOS), Prog. Polym. Sci. **36**, 1697 (2011).

[2] R. G. Larson, *The Structure and Rheology of Complex Fluids* (Oxford University Press, New York, 1999).

[3] J. Vermant and M. J. Solomon, Flow-induced structure in colloidal suspensions, J. Phys.: Condens. Matter **17**, R187 (2005).

[4] R. L. Hoffman, Discontinuous and dilatant viscosity behavior in concentrated suspensions. I. Observation of a flow instability, Trans. Soc. Rheol. **16**, 155 (1972).

[5] B. J. Ackerson, Shear induced order and shear processing of model hard sphere suspensions, J. Rheol. **34**, 553 (1990).
[6] M. D. Haw, W. C. K. Poon, and P. N. Pusey, Direct observation of oscillatory-shear-induced order in colloidal suspensions, Phys. Rev. E **57**, 6859 (1998).
[7] P. Panine, T. Narayanan, J. Vermant, and J. Mewis, Structure and rheology during shear-induced crystallization of a latex suspension, Phys. Rev. E **66**, 022401 (2002).
[8] T. H. Besseling, M. Hermes, A. Fortini, M. Dijkstra, A. Imhof, and A. van Blaaderen, Oscillatory shear-induced 3d crystalline order in colloidal hard-sphere fluids, Soft Matter **8**, 6931 (2012).
[9] N. Koumakis, A. B. Schofield, and G. Petekidis, Effects of shear induced crystallization on the rheology and ageing of hard sphere glasses, Soft Matter **4**, 2008 (2008).
[10] P. A. Smith, G. Petekidis, S. U. Egelhaaf, and W. C. K. Poon, Yielding and crystallization of colloidal gels under oscillatory shear, Phys. Rev. E **76**, 041402 (2007).
[11] R. T. Bonnecaze and M. Cloitre, in *High Solid Dispersions*, edited by M. Cloitre (Springer, Berlin, 2010), p. 117.
[12] D. Vlassopoulos and M. Cloitre, Tunable rheology of dense soft deformable colloids, Curr. Opin. Colloid Interface Sci. **19**, 561 (2014).
[13] C. Pellet and M. Cloitre, The glass and jamming transitions of soft polyelectrolyte microgel suspensions, Soft Matter **12**, 3710 (2016).
[14] J. R. Seth, L. Mohan, C. Locatelli-Champagne, M. Cloitre, and R. T. Bonnecaze, A micromechanical model to predict the flow of soft particle glasses, Nat. Mater. **10**, 838 (2011).
[15] S. E. Paulin, B. J. Ackerson, and M. S. Wolfe, Equilibrium and shear induced nonequilibrium phase behavior of PMMA microgel spheres, J. Colloid Interface Sci. **178**, 251 (1996).
[16] J.-R. Huang and T. G. Mason, Deformation, restructuring, and un-jamming of concentrated droplets in large-amplitude oscillatory shear flows, Soft Matter **5**, 2208 (2009).
[17] J. R. Huang and T. G. Mason, Shear oscillation light scattering of droplet deformation and reconfiguration in concentrated emulsions, Europhys. Lett. **83**, 28004 (2008).
[18] J. Ruiz-Franco, J. Marakis, N. Gnan, J. Kohlbrecher, M. Gauthier, M. P. Lettinga, D. Vlassopoulos, and E. Zaccarelli, Crystal-To-Crystal Transition of Ultrasoft Colloids Under Shear, Phys. Rev. Lett. **120**, 078003 (2018).
[19] F. Khabaz, T. Liu, M. Cloitre, and R. T. Bonnecaze, Shear-induced ordering and crystallization of jammed suspensions of soft particles glasses, Phys. Rev. Fluids **2**, 093301 (2017).
[20] L. Mohan, C. Pellet, M. Cloitre, and R. Bonnecaze, Local mobility and microstructure in periodically sheared soft particle glasses and their connection to macroscopic rheology, J. Rheol. **57**, 1023 (2013).
[21] M.-D. Lacasse, G. S. Grest, D. Levine, T. G. Mason, and D. A. Weitz, Model for the Elasticity of Compressed Emulsions, Phys. Rev. Lett. **76**, 3448 (1996).
[22] B. D. Lubachevsky and F. H. Stillinger, Geometric properties of random disk packings, J. Stat. Phys. **60**, 561 (1990).
[23] K. K. Liu, D. R. Williams, and B. J. Briscoe, The large deformation of a single micro-elastomeric sphere, J. Phys. D **31**, 294 (1998).
[24] P. J. Steinhardt, D. R. Nelson, and M. Ronchetti, Bond-orientational order in liquids and glasses, Phys. Rev. B **28**, 784 (1983).
[25] B. J. Ackerson and P. N. Pusey, Shear-Induced Order in Suspensions of Hard Spheres, Phys. Rev. Lett. **61**, 1033 (1988).
[26] C. R. López-Barrón, N. J. Wagner, and L. Porcar, Layering, melting, and recrystallization of a close-packed micellar crystal under steady and large-amplitude oscillatory shear flows, J. Rheol. **59**, 793 (2015).
[27] C. R. López-Barrón, D. Li, N. J. Wagner, and J. L. Caplan, Triblock copolymer self-assembly in ionic liquids: Effect of PEO block length on the self-assembly of PEO–PPO–PEO in ethylammonium nitrate, Macromolecules **47**, 7484 (2014).
[28] N. Freiberger, M. Medebach, and O. Glatter, Melting behavior of shear-induced crystals in dense emulsions as investigated by time-resolved light scattering, J. Phys. Chem. B **112**, 12635 (2008).